




# PET/MRI in Pediatric Neuroimaging: Primer for Clinical Practice

C. Pedersen,  M. Aboian,  J.E. McConathy, H. Daldrup-Link, and  A.M. Franceschi



## ABSTRACT

**SUMMARY:** Modern pediatric imaging seeks to provide not only exceptional anatomic detail but also physiologic and metabolic information of the pathology in question with as little radiation penalty as possible. Hybrid PET/MR imaging combines exquisite soft-tissue information obtained by MR imaging with functional information provided by PET, including metabolic markers, receptor binding, perfusion, and neurotransmitter release data. In pediatric neuro-oncology, PET/MR imaging is, in many ways, ideal for follow-up compared with PET/CT, given the superiority of MR imaging in neuroimaging compared with CT and the lower radiation dose, which is relevant in serial imaging and long-term follow-up of pediatric patients. In addition, although MR imaging is the main imaging technique for the evaluation of spinal pathology, PET/MR imaging may provide useful information in several clinical scenarios, including tumor staging and follow-up, treatment response assessment of spinal malignancies, and vertebral osteomyelitis. This review article covers neuropediatric applications of PET/MR imaging in addition to considerations regarding radiopharmaceuticals, imaging protocols, and current challenges to clinical implementation.

**ABBREVIATIONS:** DOPA = dioxyphenylalanine; DOTATATE = [tetraazetan-D-Phe<sup>1</sup>, Tyr<sup>3</sup>]-octreotate; FET = fluoroethyltyrosine; mFBG = meta-fluorobenzylguanidine; MIBG = metaiodobenzylguanidine; LCH = Langerhans cell histiocytosis; max = maximum; MET = methionine; SUV = standard uptake value

Serial imaging and radiation dose reduction should remain balanced in pediatric imaging. Repeat PET/CTs, especially in pediatric neuro-oncology, result in a considerable cumulative radiation dose and may increase the risk of secondary cancer.<sup>1-3</sup> The risk of radiation-induced malignancy is increased at exposures of >50–100 mSv.<sup>2</sup> A retrospective review of 78 pediatric patients found that the average cumulative dose from PET/CT during a 5-year period amounted to 78.9 mSv.<sup>3</sup> Meanwhile, reduction in the cumulative dose by PET/MR imaging has been reported to be as high as 50%–70% in pediatric lymphoma.<sup>4-6</sup> Further dose reduction may be achieved by lowering radiopharmaceutical doses with artificial intelligence–based algorithms, which is an area of active research and product development.<sup>7,8</sup>


Hybrid PET/MR imaging is particularly promising in pediatric neuroimaging because it allows functional and soft-tissue characterization with a low radiation dose and comparable agreement with PET/CT reported in several recent studies.<sup>5,6,9</sup> Unlike PET applications in body imaging, the CT component of brain PET/CT typically provides little clinically useful information beyond attenuation correction, but it does contribute to the radiation dose. PET can be used to differentiate high-grade from low-grade tumors at the initial work-up, provide prognosis for patient progression-free survival and overall survival, identify the site for optimal biopsy, and determine the extent of tumor to optimize resection and radiation therapy.<sup>10</sup> PET is also useful to evaluate tumor recurrence posttreatment in the setting of equivocal MR imaging findings and to detect transformation of tumor to a higher-grade malignancy.<sup>10</sup> MR imaging allows DWI and FLAIR sequences, which are valuable in brain tumor assessment, and also whole-body evaluation of metastatic disease.<sup>11-13</sup> MR imaging–based attenuation correction methods for PET are more complex than for CT but are possible and typically involve tissue-segmentation techniques.<sup>14</sup>

PET/MR imaging can be performed with a sequential or synchronous system. In a synchronous system, the solid-state PET detectors are located between the body and gradient coils in the 3T MR imaging gantry, which allows truly synchronous data acquisition. In a sequential system, PET and MR imaging are performed separately with transportation of the patient between scanners. A sequential system is technically easier to achieve because

Received November 2, 2021; accepted after revision December 13.

From the Department of Radiology (C.P., M.A.), Yale School of Medicine, New Haven, Connecticut; Division of Molecular Imaging and Therapeutics (J.E.M.), Department of Radiology, University of Alabama at Birmingham, Birmingham, Alabama; Department of Radiology and Pediatrics (H.D.-L.), Stanford University School of Medicine, Palo Alto, California; and Neuroradiology Division (A.M.F.), Department of Radiology, Northwell Health/Donald and Barbara Zucker School of Medicine, Lenox Hill Hospital, New York, New York.

Please address correspondence to Ana M. Franceschi, MD, Department of Radiology, 100 East 77th St, 3rd Floor, New York, NY 10075; e-mail: afranceschi@northwell.edu

 Indicates open access to non-subscribers at [www.ajnr.org](http://www.ajnr.org)

 Indicates article with online supplemental data.

<http://dx.doi.org/10.3174/ajnr.A7464>

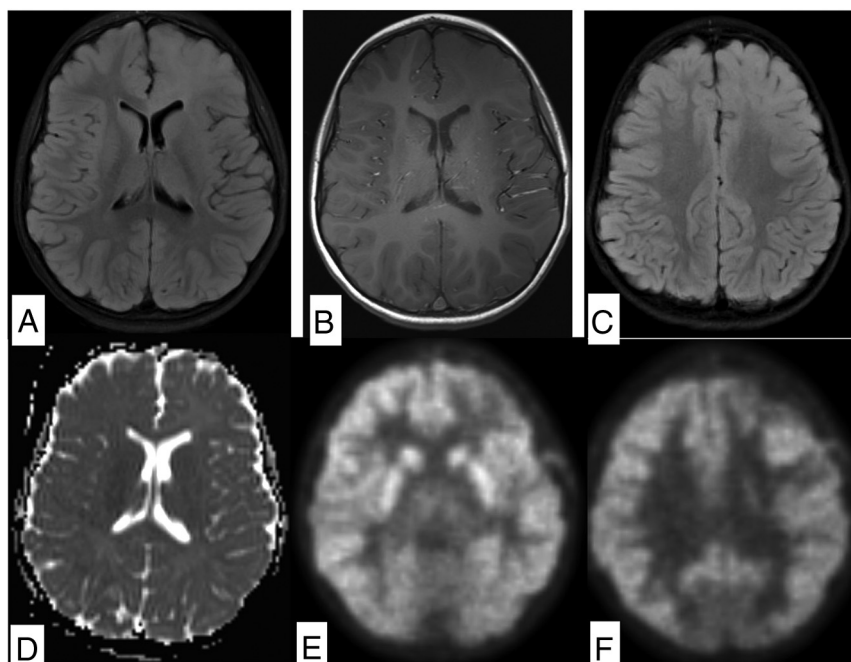


**FIGURE.** Diffuse astrocytoma in 4-year-old child demonstrates a nonenhancing FLAIR hyperintense mass involving the gray and white matter of the left frontal lobe (A and B). There is no evidence of reduced diffusion or hypointense signal on ADC (C and D). The inferior aspect of the lesion demonstrates a subtle decrease in FDG uptake compared with the contralateral side (E), while the superior portion demonstrates relative hypermetabolism on FDG-PET (F).

most US hospitals currently own separate MR imaging and PET machines, but 1 major drawback is the asynchronous nature of the scans, potentially giving rise to misregistration artifacts, longer scan times, and longer sedation requirements.<sup>15,16</sup> Therefore, a synchronous PET/MR imaging system is generally preferable in pediatric neuroimaging.<sup>4</sup>

Reduction in sedation need and sedation time is best achieved by decreasing the overall MR imaging scan time, eg, by specifically tailored protocols and sequence design.<sup>17,18</sup> In 1 study, the use of a rapid brain-tailored protocol in 1308 pediatric emergency department encounters decreased head CT use by >20% without a missed diagnosis on follow-up imaging.<sup>19</sup> Sequence design may be optimized with SyntheticMR (<https://syntheticmr.com/company/>), which allows reconstruction of multiple sequences for qualitative and quantitative analysis from a single acquisition<sup>20</sup> and has been applied to multiple disease processes including cancer, neurodegenerative disorders, and stroke.<sup>21,22</sup>

Combining PET and MR imaging results in imaging time reduction, decreases sedation time and need, and, overall, has the potential to increase throughput of scans.<sup>4</sup> Cost analysis of savings from increased throughput of patients remains an area of future investigation.

### PET/MR Imaging in Pediatric Neuro-Oncology

CNS cancer is the leading cause of death in children and adolescents.<sup>23</sup> Standard-of-care treatment for pediatric brain tumors is maximum safe resection, targeted radiation therapy, and chemotherapy. PET may help differentiate high-grade from low-grade

tumors, prognosticate progression-free and overall survival, identify an optimal biopsy site, and determine tumor extent to optimize resection and radiation therapy.<sup>10</sup> Postoperative MR imaging may be equivocal or miss small residual lesions. In this setting, PET can be used to evaluate tumor recurrence and detect transformation to a higher tumor grade.

**[<sup>18</sup>F] FDG-PET.** FDG is a positron-emitting analog of glucose that uses glucose transporters to transport labeled FDG into the cells. Once the FDG is inside the cell, it gets phosphorylated by hexokinase, resulting in intracellular retention.<sup>24</sup> This method allows imaging of cellular glucose uptake and thus allows for assessment of cellular glucose metabolism. A higher level of FDG uptake has been shown to correlate with a higher tumor grade and lead to survival prediction in primary brain tumors such as gliomas.<sup>10</sup> Disadvantages of FDG-PET include high normal brain parenchymal uptake, which may lead to poor visualization of low-grade tumors, and limitations in tumor-margin assessment (Figure). Prominent FDG uptake can also be seen in inflammatory lesions, so careful multimodal lesion evaluation is recommended.<sup>25</sup> FDG-PET is particularly valuable when differentiating posttreatment changes from tumor recurrence in the clinical setting because the former is not expected to be FDG-avid (Online Supplemental Data).<sup>24</sup>

**Amino Acid PET.** Amino acids are critical substrates in cellular metabolic pathways for synthesis of proteins and nucleotides and generation of adenosine triphosphate, all essential for cell function and growth. Up-regulation of amino acid transporters is an early step in carcinogenesis.<sup>26,27</sup> The main advantage of amino acid-based tracer imaging is very low background uptake by normal brain parenchyma, allowing better lesion detection and improved tumor-border visualization. Natural and modified amino acids have been used to study amino acid metabolism of tumors, with the most commonly used tracers including <sup>11</sup>C-methionine (MET), [<sup>18</sup>F] dioxypyphenylalanine (DOPA), [<sup>18</sup>F] fluoroethyltyrosine ([<sup>18</sup>F] FET), and [<sup>18</sup>F] fluciclovine (Online Supplemental Data).<sup>26,28,29</sup> <sup>11</sup>C-MET is a natural amino acid labeled with a carbon-11 radionuclide that has a very short half-life of 20 minutes and is, thus, limited to centers with an on-site cyclotron. The main benefit of <sup>11</sup>C-MET in pediatrics is the low radiation dose that is administered, but the inconvenience of a short half-life outweighs the benefits. [<sup>18</sup>F] FET and [<sup>18</sup>F] DOPA are modified amino acids that use the same pathway as natural amino acids but are labeled with [<sup>18</sup>F], which has led to more widespread use due to a longer half-life (110 minutes). Both tracers can be analyzed on static imaging, but interpretation of

dynamic PET is more established for [ $^{18}\text{F}$ ] FET.<sup>30,31</sup> One of the main applications of [ $^{18}\text{F}$ ] FET-PET in pediatric neuro-oncology is the definition of residual tumor after resection. In a study evaluating residual brain tumors in 27 pediatric patients, [ $^{18}\text{F}$ ] FET-PET found at least 1 residual tumor not clearly identified on MR imaging, which significantly altered management.<sup>32</sup> There are also promising results for the differentiation of radiation necrosis from tumor recurrence and the definition of tumor hypermetabolic regions, though most of the studies are performed in adults.<sup>33</sup>

[ $^{18}\text{F}$ ] FDG- and [ $^{11}\text{C}$ ] MET-PET were compared in 27 children with newly diagnosed brain tumors with diverse histology.<sup>34</sup> Twenty-two of 23 patients had increased uptake on MET-PET. High-grade tumors demonstrated a significantly elevated mean standard uptake value (SUVmean) and maximum SUV (SUVmax) compared with low-grade tumors. When the same patients were imaged with FDG-PET, 52% of tumors were hypermetabolic; 38%, eumetabolic; and 10%, hypometabolic. Because FDG uptake was higher in high-grade tumors, it was proposed that FDG-PET may provide information on tumor grade, while MET-PET provides superior information on tumor location and border delineation.

An emerging amino acid PET tracer in pediatrics [ $^{18}\text{F}$ ] fluciclovine PET, also known as Axumin PET, is an FDA-approved tracer for imaging metastatic prostate cancer, but it is also showing promising results in neuro-oncology.<sup>29,35-38</sup> It has lower background uptake compared with [ $^{11}\text{C}$ ] MET and is transported by both L-type amino acid transporter 1 and system alanine-serine-cysteine amino acid transporter-2 into the cell. Upcoming trials in pediatric brain tumors will elucidate the role and applications of this tracer in clinical neuro-oncology.

### Head and Neck Tumors

**Orbital Malignancies.** Hybrid PET/MR imaging in pediatric orbital disease is still under evaluation. Orbital involvement by lymphoma and other lymphoproliferative malignancies can be evaluated using [ $^{18}\text{F}$ ] FDG-PET, while malignancies of the optic nerves can be evaluated by both [ $^{18}\text{F}$ ] FDG and amino acid tracers.<sup>39</sup> Uveal melanoma has been described as FDG-avid, while intraorbital retinoblastoma demonstrates heterogeneous FDG avidity.<sup>39,40</sup> Meningiomas may originate along the optic nerve sheath or extend into the orbit through the sphenoid bone or foramen rotundum and can be evaluated using somatostatin receptor analogs such as gallium-68 [tetra-zetan-D-Phe1,Tyr3]-octreotate (DOTATATE).<sup>41</sup>

**Rhabdomyosarcoma in the Head and Neck.** Rhabdomyosarcoma in the head and neck region requires multimodal evaluation. The primary tumor is best evaluated with high-resolution MR imaging including noncontrast and non-fat-suppressed T1 and post-contrast T1 while [ $^{18}\text{F}$ ] FDG-PET can help delineate metastases and detect tumor recurrence (Online Supplemental Data). Recent literature indicates that FDG-PET is superior to conventional imaging in characterization of metastatic lesions and prediction of treatment response and patient outcomes.<sup>42,43</sup> Notably, chest CT is currently still required to evaluate pulmonary metastases in these patients. While MR imaging and PET are making progress, the sensitivity of CT for pulmonary metastases remains superior.

**Neuroendocrine Malignancies.** Neuroblastoma originates in primitive neural crest cells of the sympathetic nervous system and is the most common solid extracranial tumor of childhood. Most cases are diagnosed before 5 years of age and up to 50% of patients present with metastatic disease, commonly involving lymph nodes, bone, liver, and skin (Online Supplemental Data).<sup>44</sup>

Iodine-123-metaiodobenzylguanidine ( $^{123}\text{I}$ -MIBG) imaging is based on iodine accumulation in tumor cells and is the primary imaging technique for staging and treatment-response assessment and provides the foundation for targeted therapy with  $^{131}\text{I}$ -MIBG.<sup>45,46</sup>  $^{231}\text{I}$ -MIBG SPECT and SPECT/CT can be acquired advantageously to assist with tracer-uptake identification. In 1 meta-analysis,  $^{123}\text{I}$ -MIBG had lower per-lesion accuracy but was more specific compared with [ $^{18}\text{F}$ ] FDG-PET. MR imaging is a valuable for initial local staging and treatment response and lends itself well to the multivariate presentations of neuroblastoma. The sensitivity of MR imaging was superior to that of MIBG in 1 study, though less specific.<sup>47</sup> Whole-body MR imaging demonstrated good sensitivity for lymph node metastases, though with lower specificity compared with [ $^{18}\text{F}$ ] FDG-PET, partly due to difficulty in distinguishing treated and viable disease.<sup>48</sup>

More recently,  $^{124}\text{I}$ -MIBG-PET has demonstrated a favorable dosimetry profile and allows high-resolution images with increased accuracy for the detection of metastatic lesions in the head, neck, and spine compared with conventional  $^{123}\text{I}$ -MIBG SPECT in several studies.<sup>49,50</sup>

[ $^{18}\text{F}$ ] FDG-PET is generally preferred in non-MIBG-avid neuroblastomas, in aggressive and dedifferentiated tumors with loss of iodine uptake, and when high background activity complicates the evaluation of spinal involvement.<sup>51,52</sup> FDG-PET has good accuracy in metastatic lesion detection compared with  $^{123}\text{I}$  and  $^{131}\text{I}$ -MIBG scans.<sup>11,43,44</sup> Novel PET tracers such as [ $^{18}\text{F}$ ] DOPA have shown high accuracy and good agreement with MIBG in patients with relapse.<sup>53-55</sup> [ $^{18}\text{F}$ ] meta-fluorobenzylguanidine ([ $^{18}\text{F}$ ] mFBG) has been developed as a radiotracer that can provide MIBG-equivalent whole-body staging on PET/MR imaging.<sup>56,57</sup> Thus, [ $^{18}\text{F}$ ] mFBG PET/MR imaging may combine local and whole-body staging in 1 session, which is particularly helpful in pediatric patients who typically require anesthesia for medical imaging.

Additional imaging agents for neuroblastoma include  $^{68}\text{Ga}$ -DOTATATE, which is a somatostatin receptor analog approved for the detection of neuroendocrine tumors expressing somatostatin receptors such as neuroblastoma.<sup>58</sup> Somatostatin receptor analogs may be combined with peptide receptor radionuclide therapy for refractory neuroblastoma, eg,  $^{177}\text{Lu}$ -DOTATATE, because the tumor expresses somatostatin receptors, which allow select targeting.<sup>59</sup>

**Thyroid Cancer.** Thyroid nodules are less common in children than in adults but carry a higher risk of malignancy.<sup>60</sup> [ $^{18}\text{F}$ ] FDG-PET is not used routinely for thyroid nodules but may be useful in staging non-radioiodine-avid metastatic disease. MR imaging of the neck in this setting helps evaluate the thyroid resection bed for local recurrence and depicts anatomically complex regions such as the skull base and spine.<sup>60</sup>

### **PET/MR Imaging in Pediatric Spine Imaging**

[<sup>18</sup>F] FDG-PET may provide useful information in treatment-response assessment of spinal malignancies, tumor staging, and follow-up. The role of FDG-PET in neuroblastomas was covered above (Online Supplemental Data). Nononcologic spinal imaging applications of PET/MR imaging include Langerhans cell histiocytosis (LCH) and spinal infection. Furthermore, [<sup>18</sup>F] DOPA may detect hormonally active beta cells in patients with congenital hyperinsulinism.

**Pediatric Spinal Malignancy.** Astrocytomas are the most common primary intramedullary tumor in children and young adults. Most are slow-growing, low-grade tumors, while about 10%–15% are high-grade and may demonstrate elevated tracer uptake on [<sup>18</sup>F]-FDG- and <sup>11</sup>C-MET-PET. The classic imaging presentation is an eccentrically located infiltrating tumor with fusiform spinal cord expansion, variable enhancement, and often an associated cyst or syrinx. Ependymomas arise from ependymal cells of the central canal and typically present as an enhancing mass with surrounding edema, associated cysts, and hemorrhage. Due to their central location, even a small ependymoma may cause partial obstruction of the central canal and lead to formation of a syrinx.

Ewing sarcoma is the second most common primary malignant osseous tumor and typically occurs between 10 and 20 years of age. Primary vertebral Ewing sarcoma may present as either a lytic, sclerotic, or mixed lytic and sclerotic mass and may involve any part of the spine. Paravertebral Ewing sarcoma may extend directly through the neuroforamina, and spinal invasion is common.<sup>61</sup> Necrosis, cystic change, hemorrhage, and robust enhancement are common imaging findings. These tumors demonstrate avid tracer uptake on all 3 phases of technetium Tc99m methylene diphosphonate bone scans. [<sup>18</sup>F] FDG-PET may be used for staging purposes and to evaluate residual disease following treatment (Online Supplemental Data).

Sacroccygeal teratomas are the most common congenital tumor in the fetus and neonate and can be classified into 4 types depending on their location within and outside the pelvis. They are often large tumors composed of different tissues with a variable appearance on T1, T2, and postcontrast images. About a third are immature or malignant. [<sup>18</sup>F] FDG-PET may aid in staging and posttreatment follow-up of malignant sacroccygeal tumors.

### **Lymphoma**

Lymphoma is one of the most common indications for PET imaging in pediatric oncology (Online Supplemental Data). The Deauville or Lugano criteria are endorsed by the Children's Oncology Group and rely on semiquantitative measurements of glucose metabolism, which is helpful to avoid radiation therapy of non-FDG-avid residual soft-tissue masses.<sup>4</sup> Current clinical practice includes PET/CT before, during, and after initiation of therapy, with a resultant high cumulative radiation dose. Meanwhile, PET/MR imaging provides excellent soft-tissue contrast and is either equivalent or superior for malignant lymph node detection.<sup>4,62,63</sup> There is a high correlation between FDG-PET/MR imaging tumor SUV compared with PET/CT, though 1 study reported systematically lower SUVs on PET/MR imaging compared with PET/CT.<sup>4,63,64</sup> The greatest benefit of PET/MR imaging in lymphoma is radiation-dose reduction.<sup>6,64</sup> PET/MR

imaging for lymphoma in children is typically acquired as a whole-body scan from head to toe.<sup>13</sup>

### **Langerhans Cell Histiocytosis**

LCH is a proliferative process of histiocytes in children and young adults with a predilection for the vertebral bodies, which may result in vertebral body collapse (vertebra plana). The prognosis depends on disease extension, and [<sup>18</sup>F] FDG-PET is used to evaluate metastatic disease and residual tumor following resection (Online Supplemental Data).<sup>65</sup>

### **Vertebral Osteomyelitis**

Clinical manifestations of osteomyelitis are diverse and depend on location, causative microorganism, immune status, comorbidities of the host, and route of contamination. Conventional radiographs are nonspecific and only show late findings of osteomyelitis. CT provides excellent resolution and good osseous evaluation but is limited in the evaluation of soft tissues, which are commonly involved in osteomyelitis. Three-phase bone scintigraphy is based on hydroxyapatite deposition and is sensitive for detection of osteomyelitis (83%), though not specific (45%).<sup>66</sup> A leukocyte (white blood cell) scan is based on leukocyte recruitment and is more specific (88%) with reasonable sensitivity (73%) but requires cumbersome labeling of white blood cells that might not be routinely available. MR imaging and PET/CT have excellent sensitivity for vertebral osteomyelitis.<sup>67–69</sup> MR imaging provides excellent evaluation of surrounding soft tissues and is more sensitive than PET/CT for the evaluation of small epidural abscesses. FDG-PET excels in the detection of distant sites of infection. Thus, MR imaging is used as the primary imaging tool to evaluate uncomplicated unifocal cases, while FDG-PET may be considered for possible multifocal disease. PET/MR imaging fared better than PET/CT in a small study,<sup>70</sup> though larger prospective studies are yet to confirm these results.

### **Congenital Hyperinsulinism**

Congenital hyperinsulinism is characterized by persistent hypoglycemia in infancy due to abnormal insulin secretion. Genetic analysis and [<sup>18</sup>F] DOPA-PET help differentiate focal and diffuse histologic subtypes, which, in medically refractory cases, may undergo focal pancreatic resection or total pancreatectomy, respectively.

[<sup>18</sup>F] DOPA-PET is based on L-3,4-DOPA uptake in pancreatic islet cells by amino acid transporters, where it is converted to dopamine by DOPA decarboxylase.<sup>71</sup> DOPA decarboxylase activity is high in focal and diffuse forms of congenital hyperinsulinism. Thus, [<sup>18</sup>F] DOPA can be used as an indirect marker of aromatic amino acid decarboxylase activity due to the increased detection of [<sup>18</sup>F] DOPA in B-cells with a high rate of insulin synthesis and secretion.<sup>72</sup> In focal congenital hyperinsulinism, [<sup>18</sup>F] DOPA uptake is greater in the focally abnormal part of the pancreas, while diffuse forms of congenital hyperinsulinism show higher uptake in the pancreatic head compared with other parts of the pancreas. SUV suggests focal disease with >1.5-fold localized [<sup>18</sup>F] DOPA uptake compared with background pancreatic uptake.<sup>73</sup> Euglycemia must be maintained during scanning, and glucagon therapy should be stopped 2 days before scanning due to potential interference with B-cell activity.<sup>74</sup>



## CONCLUSIONS

Hybrid PET/MR imaging is a promising technique in pediatric neuroimaging and provides functional and anatomic information in combination with a reduction in the radiation dose, sedation time, and sedation events. Availability and technical implementation are still limited, but the improved diagnostic capabilities are quite attractive and applicable to a wide range of oncologic and nononcologic pediatric pathologies.

## ACKNOWLEDGMENTS

The authors would like to thank the St. Baldrick's Foundation for a research grant that supported acquisition of the PET-MR imaging images.

**Disclosure forms** provided by the authors are available with the full text and PDF of this article at [www.ajnr.org](http://www.ajnr.org).

## REFERENCES

- Mathews JD, Forsythe AV, Brady Z, et al. Cancer risk in 680,000 people exposed to computed tomography scans in childhood or adolescence: data linkage study of 11 million Australians. *BMJ* 2013;346:f2360 [CrossRef Medline](#)
- Pearce MS, Salotti JA, Little MP, et al. Radiation exposure from CT scans in childhood and subsequent risk of leukaemia and brain tumours: a retrospective cohort study. *Lancet* 2012;380:499–505 [CrossRef Medline](#)
- Chawla SC, Federman N, Zhang D, et al. Estimated cumulative radiation dose from PET/CT in children with malignancies: a 5-year retrospective review. *Pediatr Radiol* 2010;40:681–86 [CrossRef Medline](#)
- Daldrup-Link H. How PET/MR can add value for children with cancer. *Curr Radiol Rep* 2017;5:15 [CrossRef Medline](#)
- Schafer JF, et al. Simultaneous whole-body PET/MR imaging in comparison to PET/CT in pediatric oncology: initial results. *Radiology* 2014;273:220–31 [CrossRef Medline](#)
- Ponisio MR, McConathy J, Laforest R, et al. Evaluation of diagnostic performance of whole-body simultaneous PET/MRI in pediatric lymphoma. *Pediatr Radiol* 2016;46:1258–68 [CrossRef Medline](#)
- Schmall JP, Surti S, Otero HJ, et al. Investigating low-dose image quality in whole-body pediatric (18)F-FDG scans using TOF-PET/MRI. *J Nucl Med* 2021;62:123–30 [CrossRef Medline](#)
- Kaplan S, Zhu YM. Full-dose PET image estimation from low-dose PET image using deep learning: a pilot study. *J Digit Imaging* 2019;32:773–78 [CrossRef Medline](#)
- Klenk C, Gawande R, Uslu L, et al. Ionising radiation-free whole-body MRI versus F-18-fluorodeoxyglucose PET/CT scans for children and young adults with cancer: a prospective, non-randomised, single-centre study. *Lancet Oncol* 2014;15:275–85 [CrossRef Medline](#)
- Padma MV, Said S, Jacobs M, et al. Prediction of pathology and survival by FDG PET in gliomas. *J Neurooncol* 2003;64:227–37 [CrossRef Medline](#)
- Ishiguchi H, Ito S, Kato K, et al. Diagnostic performance of (18)F-FDG PET/CT and whole-body diffusion-weighted imaging with background body suppression (DWIBS) in detection of lymph node and bone metastases from pediatric neuroblastoma. *Ann Nucl Med* 2018;32:348–62 [CrossRef Medline](#)
- Maggialetti N, Ferrari C, Minoia C, et al. Role of WB-MR/DWIBS compared to 18F-FDG PET/CT in the therapy response assessment of lymphoma. *Radiol Med* 2016;121:132–43 [CrossRef Medline](#)
- Pareek A, Muehe AM, Theruvath AJ, et al. Whole-body PET/MRI of pediatric patients: the details that matter. *J Vis Exp* 2017;57:128 [CrossRef Medline](#)
- Tudisca C, Nasoodi A, Fraioli F. PET-MRI: clinical application of the new hybrid technology. *Nucl Med Commun* 2015;36:666–78 [CrossRef Medline](#)
- Brendle CB, Schmidt H, Fleischer S, et al. Simultaneously acquired MR/PET images compared with sequential MR/PET and PET/CT: alignment quality. *Radiology* 2013;268:190–99 [CrossRef Medline](#)
- Broski SM, Goenka AH, Kemp BJ, et al. Clinical PET/MRI: 2018 Update. *AJR Am J Roentgenol* 2018;211:295–313 [CrossRef Medline](#)
- Barkovich MJ, Xu D, Desikan RS, et al. Pediatric neuro MRI: tricks to minimize sedation. *Pediatr Radiol* 2018;48:50–55 [CrossRef Medline](#)
- Patel DM, Tubbs RS, Pate G, et al. Fast-sequence MRI studies for surveillance imaging in pediatric hydrocephalus. *J Neurosurg Pediatr* 2014;13:440–47 [CrossRef Medline](#)
- Ramgopal S, Karim SA, Subramanian S, et al. Rapid brain MRI protocols reduce head computerized tomography use in the pediatric emergency department. *BMC Pediatr* 2020;20:14 [CrossRef Medline](#)
- Andica C, Hagiwara A, Hori M, et al. Review of synthetic MRI in pediatric brains: Basic principle of MR quantification, its features, clinical applications, and limitations. *J Neuroradiol* 2019;46:268–75 [CrossRef Medline](#)
- Haacke EM, Chen Y, Utriainen D, et al. Strategically Acquired Gradient Echo (STAGE) imaging, part III: technical advances and clinical applications of a rapid multi-contrast multi-parametric brain imaging method. *Magn Reson Imaging* 2020;65:15–26 [CrossRef Medline](#)
- Tanenbaum LN, Tsiouris AJ, Johnson AN, et al. Synthetic MRI for clinical neuroimaging: results of the Magnetic Resonance Image Compilation (MAGiC) prospective, multicenter, multireader trial. *AJNR Am J Neuroradiol* 2017;38:1103–10 [CrossRef Medline](#)
- Siegel RL, Miller KD, Jemal A. Cancer statistics, 2020. *CA Cancer J Clin* 2020;70:7–30 [CrossRef Medline](#)
- Langbein DD, Segall GM. PET in differentiation of recurrent brain tumor from radiation injury. *J Nucl Med* 2000;41:1861–67 [Medline](#)
- Love C, Tomas MB, Tronco GG, et al. FDG PET of infection and inflammation. *Radiographics* 2005;25:1357–68 [CrossRef Medline](#)
- Youland RS, Kitange GJ, Peterson TE, et al. The role of LAT1 in (18)F-DOPA uptake in malignant gliomas. *J Neurooncol* 2013;111:11–88 [CrossRef Medline](#)
- Lu X. The role of large neutral amino acid transporter (LAT1) in cancer. *Curr Cancer Drug Targets* 2019;19:863–76 [CrossRef Medline](#)
- Dunet V, Rossier C, Buck A, et al. Performance of 18F-fluoro-ethyl-tyrosine (18F-FET) PET for the differential diagnosis of primary brain tumor: a systematic review and meta-analysis. *J Nucl Med* 2012;53:207–14 [CrossRef Medline](#)
- Albano D, Tomasini D, Bonù M, et al. (18)F-fluciclovine ((18)F-FACBC) PET/CT or PET/MRI in gliomas/glioblastomas. *Ann Nucl Med* 2020;34:81–86 [CrossRef Medline](#)
- Röhrich M, Huang K, Schrimpf D, et al. Integrated analysis of dynamic FET PET/CT parameters, histology, and methylation profiling of 44 gliomas. *Eur J Nucl Med Mol Imaging* 2018;45:1573–84 [CrossRef Medline](#)
- Zaragori T, Ginot M, Marie P-Y, et al. Use of static and dynamic [(18)F]-F-DOPA PET parameters for detecting patients with glioma recurrence or progression. *EJNMMI Res* 2020;10:56 [CrossRef Medline](#)
- Marner L, Nysom K, Sehested A, et al. Early postoperative (18)F-FET PET/MRI for pediatric brain and spinal cord tumors. *J Nucl Med* 2019;60:1053–58 [CrossRef Medline](#)
- Chiaravalloti A, Filippi L, Ricci M, et al. Molecular imaging in pediatric brain tumors. *Cancers (Basel)* 2019;11:1853 [CrossRef Medline](#)
- Utriainen M, Metsähonkala L, Salmi TT, et al. Metabolic characterization of childhood brain tumors: comparison of 18F-fluorodeoxyglucose and 11C-methionine positron emission tomography. *Cancer* 2002;95:1376–86 [CrossRef Medline](#)
- Bogsrud TV, Londalen A, Brandal P, et al. 18F-fluciclovine PET/CT in suspected residual or recurrent high-grade glioma. *Clin Nucl Med* 2019;44:605–11 [CrossRef Medline](#)

36. Henderson F, Brem S, O'Rourke DM Jr, et al. (18)F-fluciclovine PET to distinguish treatment-related effects from disease progression in recurrent glioblastoma: PET fusion with MRI guides neurosurgical sampling. *Neurooncol Pract* 2020;7:152–57 [CrossRef Medline](#)
37. Kondo A, Ishii H, Aoki S, et al. Phase IIa clinical study of [(18)F]fluciclovine: efficacy and safety of a new PET tracer for brain tumors. *Ann Nucl Med* 2016;30:608–18 [CrossRef Medline](#)
38. Michaud L, Beattie BJ, Akhurst T, et al. 18 F-Fluciclovine (18 F-FACBC) PET imaging of recurrent brain tumors. *Eur J Nucl Med Mol Imaging* 2020;47:1353–67 [CrossRef Medline](#)
39. Kalemaki MS, Karantanis AH, Exarchos D, et al. PET/CT and PET/MRI in ophthalmic oncology (Review). *Int J Oncol* 2020;56:417–29 [CrossRef Medline](#)
40. Moll AC, Hoekstra OS, Imhof SM, et al. Fluorine-18 fluorodeoxyglucose positron emission tomography (PET) to detect vital retinoblastoma in the eye: preliminary experience. *Ophthalmic Genet* 2004;25:31–35 [CrossRef Medline](#)
41. Pelak MJ, d'Amico A, Pecka KM. The prognostic usability of Ga68-DOTA-TATE PET-CT in irradiated meningioma. *Neuro-Oncology* 2016;18(Suppl 5):iv14–15 [CrossRef](#)
42. Dong Y, Zhang X, Wang S, et al. 18F-FDG PET/CT is useful in initial staging, restaging for pediatric rhabdomyosarcoma. *Q J Nucl Med Mol Imaging* 2017;61:438–46 [CrossRef Medline](#)
43. Eugene T, Corradini N, Carlier T, et al. <sup>18</sup>F-FDG-PET/CT in initial staging and assessment of early response to chemotherapy of pediatric rhabdomyosarcomas. *Nucl Med Commun* 2012;33:1089–95 [CrossRef Medline](#)
44. Berthold F, Spix C, Kaatsch P, et al. Incidence, survival, and treatment of localized and metastatic neuroblastoma in Germany 1979–2015. *Paediatr Drugs* 2017;19:577–93 [CrossRef Medline](#)
45. Bar-Sever Z, Biondani L, Shulkin B, et al. Guidelines on nuclear medicine imaging in neuroblastoma. *Eur J Nucl Med Mol Imaging* 2018;45:2009–24 [CrossRef Medline](#)
46. Mueller WP, Coppenrath E, Pfluger T. Nuclear medicine and multimodality imaging of pediatric neuroblastoma. *Pediatr Radiol* 2013;43:418–27 [CrossRef Medline](#)
47. Pfluger T, Schmied C, Porn U, et al. Integrated imaging using MRI and 123I metaiodobenzylguanidine scintigraphy to improve sensitivity and specificity in the diagnosis of pediatric neuroblastoma. *AJR Am J Roentgenol* 2003;181:1115–24 [CrossRef Medline](#)
48. Goo HW. Whole-body MRI of neuroblastoma. *Eur J Radiol* 2010;75:306–14 [CrossRef Medline](#)
49. Aboian MS, Huang Sy, Hernandez-Pampaloni M, et al. I-MIBG PET-CT to monitor metastatic disease in children with relapsed neuroblastoma. *J Nucl Med* 2021;62:43–47 [CrossRef Medline](#)
50. Huang Sy, Bolch WE, Lee C, et al. Patient-specific dosimetry using pretherapy [(1)(2)(4)I]m-iodobenzylguanidine ([[(1)(2)(4)I]mIBG) dynamic PET/CT imaging before [(1)(3)(1)I]mIBG targeted radionuclide therapy for neuroblastoma. *Mol Imaging Biol* 2015;17:284–94 [CrossRef Medline](#)
51. Papathanasiou ND, Gaze MN, Sullivan K, et al. 18F-FDG PET/CT and 123I-metaiodobenzylguanidine imaging in high-risk neuroblastoma: diagnostic comparison and survival analysis. *J Nucl Med* 2011;52:519–25 [CrossRef Medline](#)
52. Dhull VS, Sharma P, Patel C, et al. Diagnostic value of 18F-FDG PET/CT in paediatric neuroblastoma: comparison with 131I-MIBG scintigraphy. *Nucl Med Commun* 2015;36:1007–13 [CrossRef Medline](#)
53. Lopci E, Piccardo A, Nanni C, et al. 18F-DOPA PET/CT in neuroblastoma: comparison of conventional imaging with CT/MR. *Clin Nucl Med* 2012;37:e73–78 [CrossRef Medline](#)
54. Piccardo A, Lopci E, Conte M, et al. Comparison of 18F-DOPA PET/CT and 123I-MIBG scintigraphy in stage 3 and 4 neuroblastoma: a pilot study. *Eur J Nucl Med Mol Imaging* 2012;39:57–71 [CrossRef Medline](#)
55. Piccardo A, Puntoni M, Lopci E, et al. Prognostic value of (1)(8)F-DOPA PET/CT at the time of recurrence in patients affected by neuroblastoma. *Eur J Nucl Med Mol Imaging* 2014;41:1046–56 [CrossRef Medline](#)
56. Pandit-Taskar N, Zanzonico P, Staton KD, et al. Biodistribution and dosimetry of (18)F-meta-fluorobenzylguanidine: a first-in-human PET/CT imaging study of patients with neuroendocrine malignancies. *J Nucl Med* 2018;59:147–53 [CrossRef Medline](#)
57. Zhang H, Huang R, Cheung NK, et al. Imaging of the norepinephrine transporter in neuroblastoma: a comparison of [18F]-MFBG and 123I-MIBG. *Clin Cancer Res* 2014;20:2182–91 [CrossRef Medline](#)
58. Gains JE, Aldridge MD, Mattoli MV, et al. 68Ga-DOTATATE and 123I-mIBG as imaging biomarkers of disease localisation in metastatic neuroblastoma: implications for molecular radiotherapy. *Nucl Med Commun* 2020;41:1169–77 [CrossRef Medline](#)
59. Gains JE, Bomanji JB, Fersht NL, et al. 177Lu-DOTATATE molecular radiotherapy for childhood neuroblastoma. *J Nucl Med* 2011;52:1041–47 [CrossRef Medline](#)
60. Iakovou I, Giannoula E, Sachpekidis C. Imaging and imaging-based management of pediatric thyroid nodules. *J Clin Med* 2020;9:384 [CrossRef Medline](#)
61. Ilaslan H, Sundaram M, Unni KK, et al. Primary Ewing's sarcoma of the vertebral column. *Skeletal Radiol* 2004;33:506–13 [CrossRef Medline](#)
62. Lyons K, Seghers V, Sorensen JIL, et al. Comparison of standardized uptake values in normal structures between PET/CT and PET/MRI in a tertiary pediatric hospital: a prospective study. *AJR Am J Roentgenol* 2015;205:1094–101 [CrossRef Medline](#)
63. Sher AC, Seghers V, Paldino MJ, et al. Assessment of sequential PET/MRI in comparison with PET/CT of pediatric lymphoma: a prospective study. *AJR Am J Roentgenol* 2016;206:623–31 [CrossRef Medline](#)
64. Hirsch FW, Sattler B, Sorge I, et al. PET/MR in children. Initial clinical experience in paediatric oncology using an integrated PET/MR scanner. *Pediatr Radiol* 2013;43:860–75 [CrossRef Medline](#)
65. Jessop S, Crudgington D, London K, et al. FDG PET-CT in pediatric Langerhans cell histiocytosis. *Pediatr Blood Cancer* 2020;67:e28034 [CrossRef Medline](#)
66. Wang GL, Zhao K, Liu ZF, et al. A meta-analysis of fluorodeoxyglucose-positron emission tomography versus scintigraphy in the evaluation of suspected osteomyelitis. *Nucl Med Commun* 2011;32:1134–42 [CrossRef Medline](#)
67. Kouijzer IJE, Scheper H, de Rooy JWJ, et al. The diagnostic value of (18)F-FDG-PET/CT and MRI in suspected vertebral osteomyelitis: a prospective study. *Eur J Nucl Med Mol Imaging* 2018;45:798–805 [CrossRef Medline](#)
68. Termaat MF, Rajmakers PG, Scholten HJ, et al. The accuracy of diagnostic imaging for the assessment of chronic osteomyelitis: a systematic review and meta-analysis. *J Bone Joint Surg Am* 2005;87:2464–71 [CrossRef Medline](#)
69. Demirev A, Weijers R, Geurts J, et al. Comparison of [18 F]FDG PET/CT and MRI in the diagnosis of active osteomyelitis. *Skeletal Radiol* 2014;43:665–72 [CrossRef Medline](#)
70. Hulsen DJ, Geurts J, Arts JJ, et al. Hybrid FDG-PET/MR imaging of chronic osteomyelitis: a prospective case series. *Eur J Hybrid Imaging* 2019;3:7 [CrossRef Medline](#)
71. Jager PL, Chirakal R, Marriott CJ, et al. 6-L-18F-fluorodihydroxyphenylalanine PET in neuroendocrine tumors: basic aspects and emerging clinical applications. *J Nucl Med* 2008;49:573–86 [CrossRef Medline](#)
72. de Lonlay P, Simon-Carre A, Ribeiro MJ, et al. Congenital hyperinsulinism: pancreatic [18F]fluoro-L-dihydroxyphenylalanine (DOPA) positron emission tomography and immunohistochemistry study of DOPA decarboxylase and insulin secretion. *J Clin Endocrinol Metab* 2006;91:933–40 [CrossRef Medline](#)
73. Mohnike K, Blankenstein O, Minn H, et al. [18F]-DOPA positron emission tomography for preoperative localization in congenital hyperinsulinism. *Horm Res* 2008;70:65–72 [CrossRef Medline](#)
74. Ribeiro MJ, Boddaert N, Bellanné-Chantelot C, et al. The added value of [18F]fluoro-L-DOPA PET in the diagnosis of hyperinsulinism of infancy: a retrospective study involving 49 children. *Eur J Nucl Med Mol Imaging* 2007;34:2120–28 [CrossRef Medline](#)